

# Electron Beam Generated Solitary Structures in a Nonuniform Plasma System

L. Mandrake, P. L. Pritchett, and F. V. Coroniti

Department of Physics & Astronomy, University of California, Los Angeles

**Abstract.** Recent observations by the FAST satellite have identified numerous occurrences in the downward auroral current region of fast solitary structures with a characteristic size of a few local Debye lengths. We utilize a 2.5D electrostatic particle-in-cell code to investigate the generation of such structures by the interaction of narrow energetic electron beams with a gravitationally-bound exponential atmosphere. Cold, narrow electron beams are injected from both the high-altitude and low-altitude edges of the simulation domain. Both upward and downward-going beams experience a strong beam-plasma instability yielding net positive potential structures. These structures, seen to be holes in electron phase space, then accelerate or decelerate along the density gradient. For the up-going beams, the potential structures escape from the initial region of intense interaction, after which they propagate surprisingly far. The down-going structures accelerate but become degraded and break up due to the finer scales present in the increased density region. The gradient-dependent acceleration therefore selects upward-going structures as likely to be more robust in the auroral region.

## 1. Introduction

Large-amplitude solitary waves with speeds much greater than the ion acoustic speed have been observed in many regions of the terrestrial magnetosphere: in the plasma sheet boundary layer [Matsumoto et al., 1994; Omura et al., 1996], at bow shock crossings [Matsumoto et al., 1997; Bale et al., 1998], in the middle and high altitude auroral zone [Mozer et al., 1997; Franz et al., 1998; Cattell et al., 1999], and most recently by the FAST satellite in the lower auroral region between 2000 and 4000 km [Ergun et al., 1998a, 1998b]. The FAST observations demonstrate that these solitary structures are common features of the auroral downward current region, that they are associated with quasistatic, magnetic-field-aligned electric fields of large amplitude (up to 2.5 V/m) with a characteristic size of a few Debye lengths, and that they can be described as a traveling BGK electron hole [Muschiatti et al., 1999].

Many features of the solitary structures can be explained in terms of the linear and nonlinear evolution of counter-streaming cold electron beam instabilities [Omura et al., 1996; Mottez et al., 1997; Miyake et al., 1998; Goldman et al., 1999]. Typically, these studies involve particle-in-cell (PIC) simulations in idealized configurations which do not incorporate any of the structure of the auroral zone plasma and in which there is no distinction between propagation of the solitary structures parallel as opposed to anti-parallel along the magnetic field. In the present investigation we perform PIC simulations in a more realistic model which includes the strong density variation of the ambient plasma with altitude in the auroral region. We find that

the behavior of the electron beam generated potential structures is strongly affected by the density gradient and that the properties of the upward traveling structures at distances far from the injection region approach those seen in the FAST observations.

## 2. Simulation Model

We employ an electrostatic PIC simulation model with two spatial dimensions ( $x, z$ ) and all three velocity components to represent the upper region of the ionosphere. The cold ionosphere is represented by a gravitationally bound plasma atmosphere in which the electron and ion densities are perfectly matched and have an exponentially decreasing density with respect to height (Figure 1). The separation of masses that would normally result from the gravitational force is opposed by an external, static, ambipolar electric field. The positive  $z$  direction is directed upward, and the uniform magnetic field points downward. Poisson's equation is solved assuming that the internally generated self-consistent potential  $\Phi$  (whose source excludes that of the external static field) vanishes at the upper and lower  $z$  boundaries and obeys periodic boundary conditions in  $x$ . At the upper and lower boundaries particles are free to exit from the system, while new particles are injected based on the thermal distributions. This system proves to be remarkably stable, with the total particle number and average temperature varying by less than 0.4% over an interval  $\omega_{pe}T=5000$ , where  $\omega_{pe}$  is the average plasma frequency. Additional particle species that can be included are a warm magnetospheric plasma and a narrow, cold electron beam that can be injected at either the top or bottom of the simulation region; these added populations experience only the self-consistent fields, not the external gravitational or atmospheric ambipolar forces.

In the present simulations we inject a field-aligned stream of cold electrons  $6\Delta$  wide into a purely ionospheric background plasma whose density variation from top to bottom is a factor of 10. In the run labeled DOWN, the beam is injected from the top of the box (low density end), whereas in the run labeled UP, the beam is injected from the bottom (high density end). For comparison, an additional run, labeled FLAT, is performed in which the beam is injected at the bottom into a uniform plasma without a density gradient (see Figure 1). In the DOWN run, the beam and background begin with equal densities, whereas in the UP case the beam has one-tenth of the initial background density. The simulation grid is  $N_x \times N_z = 64 \times 512$  or  $64 \times 1024$ , where the grid spacing  $\Delta$  is related to the average background Debye length by  $\lambda_{De} = 1.14 \Delta$  (Table 1). The electron beam has a width of  $6\Delta$ , and the initial drift speed is  $4 v_{Te}$ , where  $v_{Te}$  is the background electron thermal velocity. The magnetic field strength is such that  $\Omega_e/\omega_{pe} = 2$  at  $z=188$ , where  $\Omega_e$  is the electron cyclotron frequency, and the ion to electron mass ratio is  $m_i/m_e = 64$ . The ratio  $T_e/T_i = 1$ . The time step is  $\omega_{pe}\Delta t = 0.08$ , and the total number of particles is  $\sim 9.0 \times 10^6$ . A typical run lasts about 10,000 timesteps.

## 3. Results

In all runs (DOWN, UP, FLAT), the injected cold electron beam is seen to experience a strong convective beam-plasma

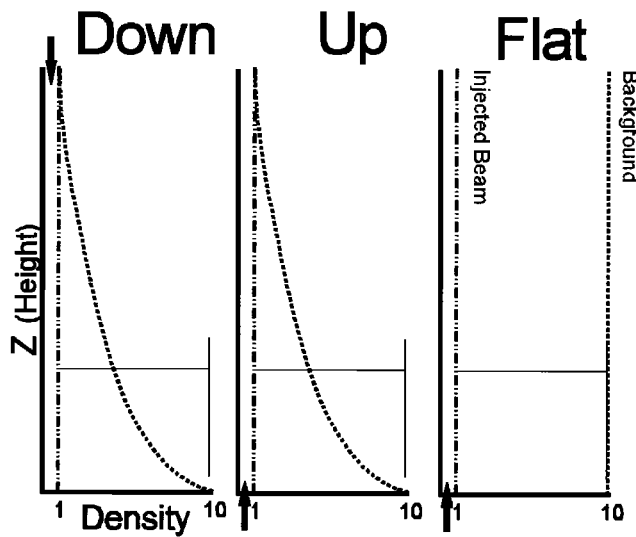


**Figure 1.** Beam direction and density relative to background populations.

instability as expected (Figure 2). The net charge of the injected beam causes the background electrons to begin evacuation of the field lines occupied by the beam. Charge separation structures develop within the beam with longitudinal size scale consistent

**Table 1.** Run parameters

Population	$\beta$	$1/\Omega_e$	$1/\omega_p$	$v_d$	$r_{gro}$	$\lambda_D$
e- (back)	5e-4	6.0	12.0	0	0.57	1.14
i+ (back)	5e-4	384	96.0	0	4.50	1.14
e- (beam)	1.6e-7	6.0	29.9	4	.025	0.13

Inverse frequencies in terms of timesteps, velocities in terms of background electron thermal velocity, and distances in terms of simulation cells.

with  $\omega/k = v_{hole}$ , where  $\omega$  is near the local electron plasma frequency, and  $v_{hole} (\sim 3 v_{Te})$  is the mean drift speed of the structure. These structures are seen to be electron holes in phase space ( $v_z$  vs.  $z$ ) where electron trapping has terminated the exponential growth of the linear instability. The lack of beam electron density in the holes produces a net positive potential structure with an associated bipolar parallel electric field. The amplitude of these potential structures can reach the thermal energy of the background electrons (Figure 3). As the beam electrons bounce in their trapped oscillations, there is some slippage from perfect orbits that result in fine beamlets emitted from each vortex (Figure 2, UP run,  $z=75$ ). A counter-streaming current is therefore established made up of those electrons released during retrograde movement. This back-streaming

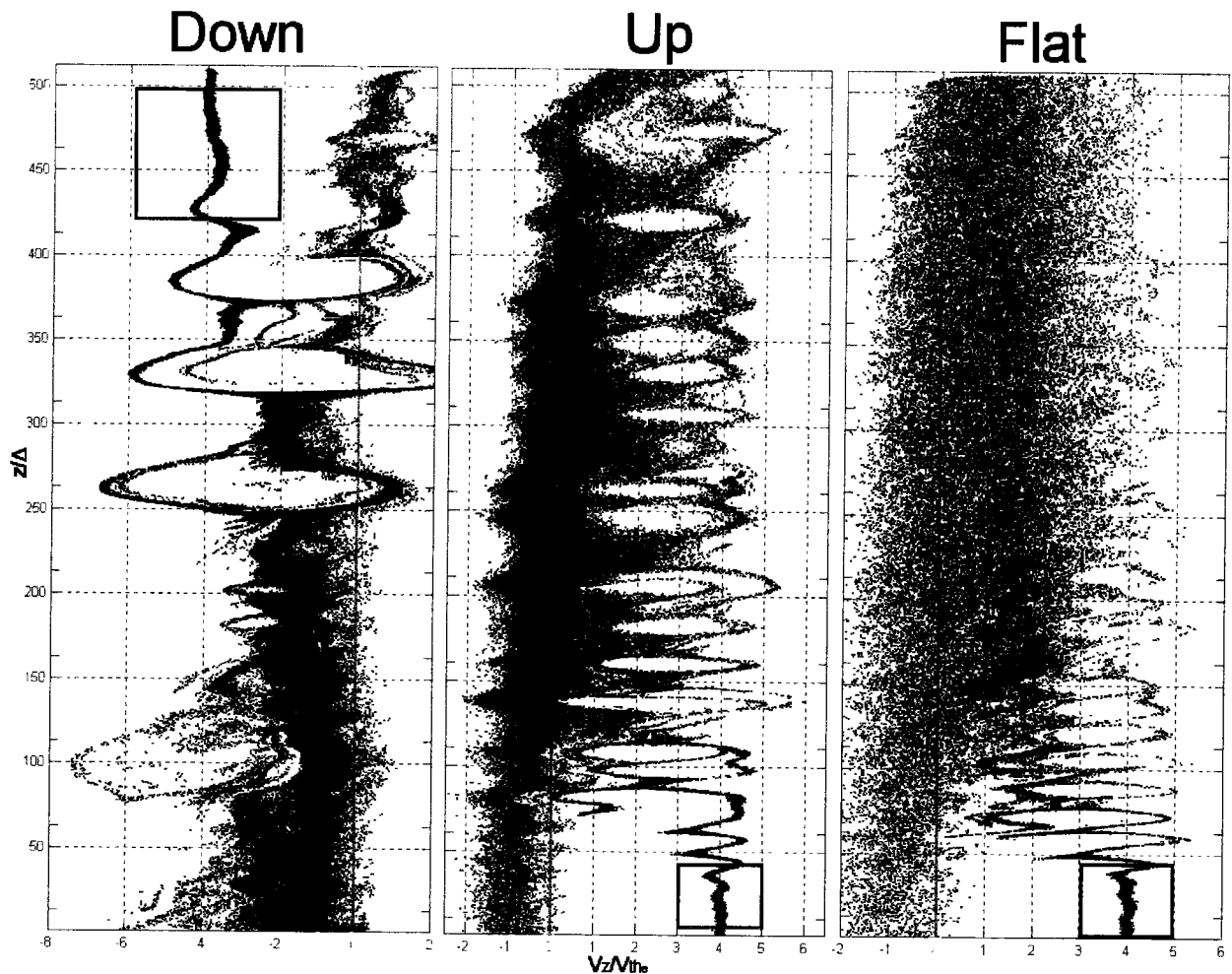


**Figure 2.** Phase space plots of  $Z$  vs.  $V_z$  taken at a single timestep near the end of the simulation for beam electrons only. The box in each graph shows the injection region where linear fluid theory predicts the frequency and size scale of the initial oscillation.

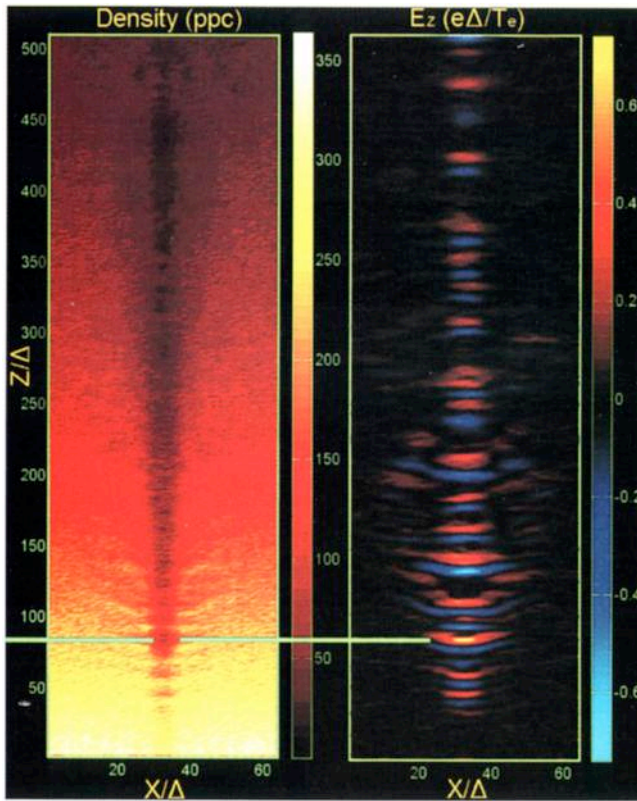


**Figure 3.** The background (not beam) electron density and parallel electric field in the UP run. The horizontal marker denotes where beam density has exceeded background density.

current can become strong enough to itself produce vortices. However, divergence from standard beam-plasma theory commences as the phase holes continue to propagate along the density gradient; in all cases, a net acceleration towards the denser region of the background electron population is observed that is strongly dependent on the amplitude of the potential structures.

In the UP run, the vortices are decelerated by this density-seeking effect, with larger structures being decelerated faster than smaller structures. This causes continual collisions and interactions along the beam which produce rich “triple holes” (e.g. Figure 2,  $z=450$ ,  $z=210$ ) and other exotic phase space arrangements. Remarkably, such complex structures remain coherent as they move through the regions of ever decreasing density. Typical interactions of these phase space holes include bypass without grievous distortion if the velocities are sufficiently disparate or merger if the velocities are similar. Smaller holes are generally destroyed by larger holes, and holes may increase or decrease in size through merger interactions. The surprising robustness of these coherent structures is due to the ease with which the beam expels background electrons and thus creates a pronounced channel as it emerges into sparser and sparser density regions (Figure 3). In this run, the beam strongly interacts with the background population until, within  $\sim 100 \Delta$  of its injection, the background electron density has been reduced below the beam density and contributes no further structure.

In the DOWN run, the size scale of the electron phase space holes is much larger, as is expected due to the lower background plasma frequency of the sparse injection region. These large structures then experience strong acceleration down the field lines, quickly reaching mean speeds greater than any thermal or

drift velocity in the initial system. However, as they enter regions of ever-increasing background density, the coherence of the structures is degraded far more rapidly than in the UP case. Since the acceleration and initial velocities have the same sign, vortex merging is unlikely in this case; any interacting vortices will likely have greatly disparate velocities. In the higher density regions at lower altitude, the beam is unable to expel sufficient background electrons to create a channel with density below the beam density; hence, the structures degrade rapidly.

In the FLAT run, the same initial conditions are used as in the UP run, except that no gradient exists. The trapped electron vortices form and then are immediately destroyed by continued intense interaction with the background plasma. Without the gradient, the beam cannot drain its magnetic field lines of background electrons, the vortices cannot escape the region of interaction, and hence no bipolar structures propagate.

The spacing between successive solitary pulses in the FAST observations is typically about 1 ms, corresponding to  $\sim 20 f_{pe}^{-1}$  [Ergun et al., 1998b]. Initially, the spacing in the simulations is small compared to this value, though by the end of the box both runs approach a similar value (Figure 4). In both runs with a density gradient, mechanisms exist to provide for increased spacing. In the DOWN run, acceleration of each vortex provides a continually increasing mean spatial distance between individual cores. In the UP run, one might expect spacing to decrease. This in fact occurs as a transient effect. However, as phase space holes collide, mergers are frequent thus reducing the density of vortices and increasing their spacing. Therefore, either by direct acceleration or via hole-hole condensation, these structures tend to space out as they propagate.

The major current of the system is simply the injected electron beam (Figure 5). The vortices serve to transfer momentum to the background electron population, gradually reducing the beam's current contribution and increasing a parallel current in the background. The ions weakly oppose the current flow. In all cases, the background ion density was enhanced along the beam channel to assist charge neutralization.

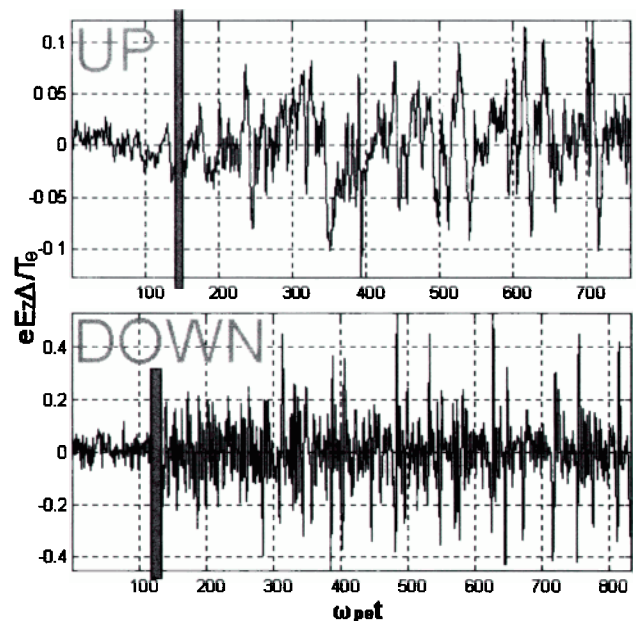


**Figure 4.** Parallel electric field signatures near the exit of the box throughout the run. The vertical grey bar shows the time at which the primary electron beam reached the observed location with significant density. Note the differing axes on the plots. UP run was recorded at  $Z=412$ ,  $X=32$ , while DOWN was recorded at  $Z=100$ ,  $X=32$ .

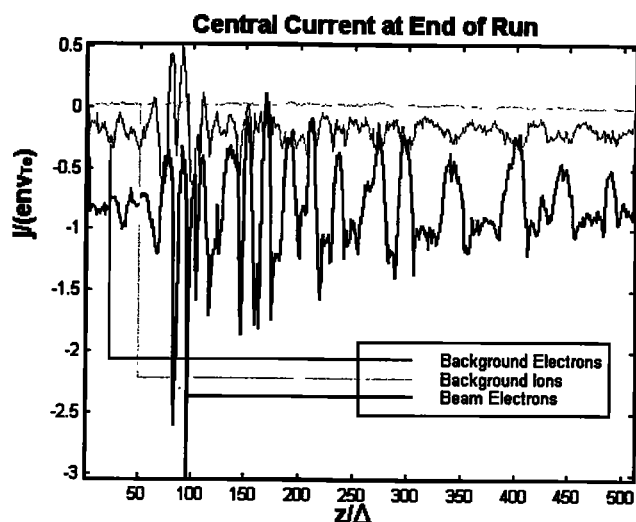


Figure 5. Current carried along the beam by all three populations for UP run.

#### 4. Discussion

The FAST observations have shown that fast solitary structures are a common feature of the downward current region in the auroral zone between 2000 and 4000 km. These structures have been shown to be three-dimensional electron phase space holes traveling at approximately the electron drift velocity and to have a characteristic spatial scale of a few Debye lengths. In the present investigation, we have used an electrostatic simulation model which includes a strong density variation along the magnetic field to examine how such structures can arise from the interaction between an electron beam and the ambient plasma. The density variation was found to play a crucial role in determining the nature of the structures that propagate away from the initial interaction region. In a uniform plasma, the beam-generated vortices are rapidly destroyed. For beam injection into an increasing density (which models the upward auroral current region), the vortices are accelerated toward the denser background plasma. There is little interaction between individual vortices, and the vortices become degraded due to the interaction with the increasing background density. For injection into a decreasing density (the downward auroral current region), there is a complex series of interactions between vortices which produce bipolar structures that remain coherent as they propagate along a channel created in the regions of ever decreasing density.

The present model clearly omits a number of significant effects. First, the mechanism for generating the electron beams has not been addressed. Next, the size of the simulation system and the total density variation are much smaller than the corresponding auroral parameters. The local Debye length as observed by FAST is  $\sim 80$  m, and thus the height of our simulation region corresponds to only 40–80 km. One needs to verify that the bipolar structures can remain coherent over many thousands of km. The gradient in magnetic field strength has also been neglected, but its inclusion should further favor the upgoing

beam case: an anti-mirror effect will further augment the field-aligned nature of the beam, whereas for downgoing beams the mirror force will tend to diffuse the beam in pitch angle. Despite these limitations, it seems clear that the density gradient in the auroral region should play a crucial role in the evolution of solitary structures, and the present simulation results provide a plausible explanation for the observed disparity in the bipolar structures between the upward and downward auroral current regions.

**Acknowledgments.** We thank R. J. Strangeway for an informative discussion regarding the FAST observations. This work was supported by NASA grants NAG5-8059 and NAG5-8132.

#### References

- Bale, S.D., P.J. Kellogg, D.E. Larson, R.P. Lin, K. Goetz, and R.P. Leppin, Bipolar electrostatic structures in the shock transition region: evidence of electron phase space holes, *Geophys. Res. Lett.*, **25**, 2929–32, 1998.
- Cattell, C.A., et al., Comparisons of Polar satellite observations of solitary wave velocities in the plasma sheet boundary and the high altitude cusp to those in the auroral zone, *Geophys. Res. Lett.*, **26**, 425–8, 1999.
- Ergun, R.E., et al., FAST satellite observations of large-amplitude solitary structures, *Geophys. Res. Lett.*, **25**, 2041–4, 1998a.
- Ergun, R.E., C.W. Carlson, J.P. McFadden, F.S. Mozer, L. Muschietti, I. Roth, and R.J. Strangeway, Debye-scale plasma structures associated with magnetic-field-aligned electric fields, *Phys. Rev. Lett.*, **81**, 826–9, 1998b.
- Franz, J.R., P.M. Kintner, and J.S. Pickett, POLAR observations of coherent electric field structures, *Geophys. Res. Lett.*, **25**, 1277–80, 1998.
- Goldman, M.V., M.M. Oppenheim, and D.L. Newman, Nonlinear two-stream instabilities as an explanation for auroral bipolar wave structures, *Geophys. Res. Lett.*, **26**, 1821–4, 1999.
- Matsumoto, H., H. Kojima, T. Miyatake, Y. Omura, M. Okada, I. Nagano, and M. Tsutui, Electrostatic solitary waves (ESW) in the magnetotail: BEN wave forms observed by GEOTAIL, *Geophys. Res. Lett.*, **21**, 2915–18, 1994.
- Matsumoto, H., H. Kojima, Y. Kasaba, T. Miyake, R. R. Anderson, and T. Mukai, Plasma waves in the upstream and bow shock regions observed by GEOTAIL, *Adv. Space Res.*, **20**, 683–93, 1997.
- Miyake, T., Y. Omura, H. Matsumoto, and H. Kojima, Two-dimensional computer simulations of electrostatic solitary waves observed by Geotail spacecraft, *J. Geophys. Res.*, **103**, 11841–50, 1998.
- Mottez, F., S. Perraut, A. Roux, and P. Louarn, Coherent structures in the magnetotail triggered by counterstreaming electron beams, *J. Geophys. Res.*, **102**, 11399–408, 1997.
- Mozer, F.S., R. Ergun, M. Temerin, C. Cattell, J. Dombeck, and J. Wygant, New features of time domain electric-field structures in the auroral acceleration region, *Phys. Rev. Lett.*, **79**, 1281–4, 1997.
- Muschietti, L., R.E. Ergun, I. Roth, and C.W. Carlson, Phase-space electron holes along magnetic field lines, *Geophys. Res. Lett.*, **26**, 1093–6, 1999.
- Omura, Y., H. Matsumoto, T. Miyake, and H. Kojima, Electron beam instabilities as generation mechanism of electrostatic solitary waves in the magnetotail, *J. Geophys. Res.*, **101**, 2685–97, 1996.

L. Mandrake, P. L. Pritchett, and F. V. Coroniti, Department of Physics & Astronomy, University of California, Los Angeles, CA 90095  
(e-mail: mandrake@physics.ucla.edu)

(Received March 23, 2000; revised May 18, 2000; accepted June 27, 2000.)